# Vibrational Studies and Microwave Dielectric Properties of A-Site-Substituted Tellurium-Based Double Perovskites

Anderson Dias,*,† Ganesanpotti Subodh,‡ Mailadil T. Sebastian,‡ Márcio M. Lage,§ and Roberto L. Moreira§

*Departamento de Química, Universidade Federal de Ouro Preto, Campus Morro do Cruzeiro, ICEB II, Ouro Preto-MG, 35400-000, Brazil, Materials and Minerals Division, National Institute for Interdisciplinary Science and Technology, Trivandrum-695 019, India, and Departamento de Física, Universidade Federal de Minas Gerais, C.P. 702, Belo Horizonte-MG, 30123-970, Brazil*

*Received February 2, 2008. Revised Manuscript Received April 2, 2008*

$A_2MgTeO_6$ (A = Ba, Sr, Ca) ceramics were prepared by solid-state route and their microstructure and microwave dielectric properties, as well as the vibrational phonon modes were investigated using the resonance method and spectroscopic techniques for the first time. For the optimized sintering temperatures, $Ba_2MgTeO_6$, $Sr_2MgTeO_6$, $Ca_2MgTeO_6$ materials presented the following properties: $\varepsilon_r$ of 11, 14.3, and 13.2; $Q_u$xf of 25, 27.5, and 81 THz, and $\tau_f$ of −16, −61, and −81 ppm/°C, respectively. XRD besides Raman and infrared spectroscopies were employed to investigate the structures of these materials and the results showed that Ba- and Sr-based double perovskites belong to the tetragonal *I*4/*m* space group, while Ca-based materials exhibit a monoclinic $P2_1/n$ structure. The phonon modes were evaluated and the intrinsic microwave dielectric properties were discussed in terms of the A-site substitution on tellurium-based ceramics. The number of bands observed in both spectroscopic techniques agrees well with the group-theoretical predictions for all materials, thus confirming our assumptions.

## Introduction

Among thousands of processed inorganic materials, ceramics with the perovskite structure dominate the world of useful compounds because of their well-known versatility.[1] From the point of view of materials chemistry, these ceramics present an incredibly wide array of structures and phases with totally different functions, which are directly related to the combination of chemical elements in the basic formula $ABX_3$. The multiple ion substitution in the perovskite lattice in either A and B positions, or in both, creates the so-called complex perovskites, which present pairs of unlike valence cations in proportions depending on their oxidation states and ionic radii.[1] In the last 50 years, a huge number of "old" and "new" compounds are being studied by a wide scientific community in the framework of their crystal chemistry toward emerging applications: ferroelectrics,[2] superconductors,[3] relaxors,[4] photonics,[5] catalysts,[6] and microwave dielectrics.[7]

Today, the ever-growing proliferation in telecommunication technologies makes an increasing demand for microwave dielectric ceramics.[7,8] These materials are the prime components in various communication and microwave systems, which require high dielectric constants ($\epsilon_r$) for size reduction, minimum possible dielectric losses, and near-zero temperature stability of the resonant frequency ($\tau_f$). Even though a number of microwave resonator materials are available, the demand for new microwave dielectrics with the multifunctionality feature is also increasing.[7] In this respect, complex perovskites provide a wide and best range of suitable materials because of open possibilities of tailoring the chemistry and consequently the parameters to meet the device requirements. It is well-known that the final properties are highly dependent on the nature of the cations present as well as on the structural features, including ordering and defects.[9]

Extensive research has been carried out to investigate the properties of complex $A(B'_{1/3}B''_{2/3})O_3$ perovskites, such as $Ba(Mg_{1/3}Ta_{2/3})O_3$ and $Ba(Zn_{1/3}Ta_{2/3})O_3$, as they possess excellent microwave properties.[10] Despite that, less attention has been paid to microwave dielectric properties of $A(B'_{1/2}B''_{1/2})O_3$, known as "double perovskites". Current investigations on these ceramics[11,12] showed a number of temperature-stable microwave dielectric ceramics with relative permittivity greater than 20. Also, new applications

* Corresponding author. Tel. 55-31-3559-1716. E-mail: anderson_dias@iceb.ufop.br.
† Universidade Federal de Ouro Preto.
‡ National Institute for Interdisciplinary Science and Technology.
§ Universidade Federal de Minas Gerais.

(1) Mitchell, R. H. *Perovskites modern and ancient*; Almaz Press: Ontario, 2002. Tejuca, L. G., Fierro, J. L. G., Eds. *Properties and applications of perovskite type oxides*; Marcel Decker: New York, 1993.
(2) Samara, G. A. *J. Phys.: Condens. Matter* **2003**, *15*, R367.
(3) Blackstead, H. A.; Dow, J. D.; Harshman, D. R.; Yelon, W. B.; Chen, M. X.; Wu, M. K.; Chen, D. Y.; Chien, F. Z.; Pulling, D. B. *Phys. Rev. B* **2001**, *61*, 214412–1.
(4) Bokov, A. A.; Ye, Z. G. *J. Mater. Sci.* **2006**, *41*, 31.
(5) Wojtowicz, A. J.; Drozdowski, W.; Wisniewski, D.; Lefaucheur, J. L.; Galazka, Z.; Gou, Z. H.; Lukasiewicz, T.; Kisielewski, J. *Opt. Mater.* **2006**, *28*, 85.
(6) Osterloh, F. E. *Chem. Mater.* **2008**, *20*, 35.
(7) Reaney, I. M. Iddles, D. *J. Am. Ceram. Soc.* **2006**, *89*, 2063.
(8) Subodh, G.; James, J.; Sebastian, M. T.; Paniago, R.; Dias, A.; Moreira, R. L. *Chem. Mater.* **2007**, *19*, 4077.
(9) Knapp, M. C.; Woodward, P. M. *J. Solid State Chem.* **2006**, *179*, 1076.
(10) Varma, M. R.; Raghunandan, R.; Sebastian, M. T. *Jpn. J. Appl. Phys.* **2005**, *44*, 298.
(11) Khalam, L. A. and M. T. Sebastian. *Int. J. Appl. Ceram. Technol.* **2006**, *3*, 364.
(12) Khalam, L. A.; Sebastian, M. T. *J. Am. Ceram. Soc.* **2007**, *90*, 1467.

10.1021/cm8003326 CCC: $40.75 
Published on Web 06/10/2008

extended the working frequency region toward the millimeter-wave range because of shortage of conventional frequency range.[13] More recently, studies have been performed on double perovskites with hexavalent cations, such as Mo, Re, W, and Te.[14–20] According to Augsburger et al.,[18] p-elements like tellurium can be successfully stabilized in B-sites of the perovskite structure, showing the required spherical symmetry and adequate ionic size. Previous work on Te-based compositions showed excellent microwave properties with very low sintering temperatures (>700 °C).[13,21] Even though a number Te-based new materials are reported, to the best of our knowledge, no investigation has been carried out to explore the microwave dielectric (MW) properties of complex perovskites with Mg and Te in their composition.

Also, the ceramics with the formula $A_2MgTeO_6$ (A = Ba, Sr, Ca) were not yet investigated in the perspective of the behavior of their polar phonon modes (intrinsic contributions, depending on the crystalline structure). In order to study the potential of a given material to MW applications (resonators or filters), the knowledge of its polar phonons features is thus mandatory. From the point of view of crystal chemistry, Bayer[22] reported for the first time the existence of the compounds $A_2MgTeO_6$ (Sr, Pb, Ba), in which Te is oxidized to the hexavalent state and forms stable perovskite structures with space group $Fm\bar{3}m$ (No. 225). He also predicted a noncubic symmetry for the $Ca_2MgTeO_6$ ceramics. Recently, Ayala et al.[23] studied the characteristics of the optical phonons in $A_2CoTeO_6$ (A = Sr and Ca) materials based on Raman scattering data and found correlations between structures and vibrational modes for these ceramics. In the present work, the microstructure and microwave dielectric properties, besides the phonon modes of chemically substituted $A_2MgTeO_6$ samples (A = Ba, Sr, Ca) were investigated in detail. Raman and infrared spectroscopies were employed together with group-theory calculations, and the results allowed us to contribute to the debate on the crystalline structure and MW properties of this ceramic system.

## Experimental Section

$A_2MgTeO_6$ (A = Ba, Sr, and Ca) ceramics were prepared by solid-state ceramic route. High purity $CaCO_3$, $SrCO_3$, $BaCO_3$, and $TeO_2$ (99+%, Aldrich Chemical Co.) were used as the starting materials. Stoichiometric amounts of powder mixtures were ball-milled in distilled water medium using yttria-stabilized zirconia balls in a plastic container for 24 h. The slurry was dried, ground well, heated at a rate of 2.5 °C/min, and kept at 700 °C for 4 h. A slow heating rate was used for the oxidation of $Te^{4+}$ to $Te^{6+}$, which occurs only when certain thermodynamic conditions are satisfied.[24] The mixed powders were calcined at 1080 °C for 4 h, ground into fine powders, and divided into different batches for optimizing sintering temperature. Because of the poor sinterability of the $A_2MgTeO_6$, 0.2 wt% $B_2O_3$ (Aldrich Chemical Co.) was added as a sintering aid and mixed thoroughly to the powders in distilled water and dried. They were then mixed with 4 wt% of polyvinyl alcohol (molecular weight ≈ 22000, BDH Laboratory Suppliers, England) and again dried and ground well. Cylindrical pucks of about 10−11 mm height and about 20 mm diameter were made by applying a pressure of 150 MPa. These compacts were then fired at 600 °C for 30 min to expel the binder before sintering at temperatures ranging from 1175 to 1300 °C for 4 h. Bulk densities of the sintered samples were measured using the Archimedes's method.

The crystal structure and phase purity of the powdered samples were studied by X-ray diffraction technique (XRD) using Cu Kα radiation ($\lambda$ = 0.15418 nm) in a Philips diffractometer, with a graphite monochromator and a nickel filter in the $2\theta$ range 10−100° (step 0.06°$2\theta$). Relatively high-resolution data to be used in investigations concerning deviations from cubic symmetry were collected using a Shimadzu D-6000 diffractometer operating with Fe Kα radiation ($\lambda$ = 0.19360 nm) over particular ranges using special conditions of 15 s/step of 0.01°$2\theta$. However, imperfect monochromation introduced, in these cases, a contribution of $K\alpha_2$, which was allowed for the data analysis. The sintered samples were thermally etched for 20 min at temperatures 25 °C below the sintering temperature, and the microstructures were analyzed by using a scanning electron microscope (JEOL-JSM 5600 LV, Tokyo, Japan). The microwave dielectric properties were measured by a Vector Network Analyzer (8753 ET, Agilent Technologies). The dielectric constants and unloaded quality factors of the samples were determined, respectively, by Hakki and Coleman[25] and cavity methods[26] in the frequency range 4−6 GHz. The specimen was placed on a low-loss quartz spacer inside a copper cavity, with a silver plated inner side. The use of the low-loss single crystal quartz spacer reduces the effect of losses due to the surface resistivity of the cavity. The diameter of the cavity was about 4 times larger than that of the sample for better isolation of the excited $TE_{01\delta}$ mode. The $\tau_f$ were measured by noting the variations of $TE_{01\delta}$ mode frequency with the temperature in the range 25 to 75 °C.

Raman spectra were collected in back-scattering configuration by using an Olympus confocal microscope attached to a triple-monochromator Dilor XY spectrometer (objective 80×). The 514.5 nm line of an $Ar^+$ laser (effective 2 mW at the sample's surface) was used as the exciting line, and a liquid-$N_2$-cooled charge-coupled device (CCD) detected the scattered light. The frequency resolution was better than 2 $cm^{-1}$, and the accumulation times were typically three collections of 180s. The obtained spectra were divided out by the Bose−Einstein thermal factor[27] before being fitted by a sum of Lorentzian lines. Infrared reflectivity spectra were recorded in a Fourier-transform spectrometer (Bomem DA 8−02) equipped with

(13) Subodh, G.; Sebastian, M. T. *J. Am. Ceram. Soc.* **2007**, *90*, 2266.
(14) Patwe, S. J.; Achary, S. N.; Mathews, M. D.; Tyagi, A. K. *J. Alloys Compd.* **2005**, *390*, 100.
(15) Patwe, S. J.; Achary, S. N.; Mathews, M. D.; Tyagi, A. K. *Mater. Chem. Phys.* **2006**, *98*, 486.
(16) Yang, J. H.; Choo, W. K.; Lee, C. H. *Acta Crystallogr., Sect. C: Cryst. Struct. Commun.* **2003**, *59*, i86.
(17) Iwanaga, D.; Inaguma, Y.; Itoh, M. *Mater. Res. Bull.* **2000**, *35*, 449.
(18) Augsburger, M. S.; Viola, M. C.; Pedregosa, J. C.; Carbonio, R. E.; Alonso, J. A. *J. Mater. Chem.* **2006**, *16*, 4235.
(19) Augsburger, M. S.; Viola, M. C.; Pedregosa, J. C.; Munoz, A.; Alonso, J. A.; Carbonio, R. E. *J. Mater. Chem.* **2005**, *15*, 993.
(20) Ortega-San Martin, L.; Chapman, J. P.; Lezama, L.; Garitaonandia, J. J. S.; Marcos, J. S.; Rodriguez-Fernandez, J.; Arriortua, M. I.; Rojo, T. *J. Mater. Chem* **2006**, *16*, 66.
(21) Kwon, D. K.; Lanagan, M. T.; Shrout, T. R. *Mater. Lett.* **2007**, *61*, 1827.
(22) Bayer, G. *J. Am. Ceram. Soc.* **1963**, *46*, 604.
(23) Ayala, A. P.; Guedes, I.; Silva, E. N.; Augsburger, M. S.; Viola, M. C.; Pedregosa, J. C. *J. Appl. Phys.* **2007**, *101*, 123511.
(24) Sudarsan, K. G.; Dindi, S. N. *Prog. React. Kinet. Mech.* **2002**, *27*, 127.
(25) Hakki, B. W.; Coleman, P. D. *IEEE Trans. Microwave Theory Technol.* **1960**, *8*, 402.
(26) Krupka, J.; Derzakowski, K. D.; Riddle, B.; Jarvis, J. B. *Meas. Sci. Technol.* **1998**, *9*, 1751.
(27) Hayes W.; Loudon, R. *Scattering of light by crystals*; Wiley: New York, 1978.

**Table 1. Density and Microwave Dielectric Properties of $A_2MgTeO_6$ (A = Ba, Sr, or Ca) Materials as Functions of Sintering Temperature**

| | density (g/cm$^3$) | | | $\varepsilon_r$<br>$Q_u$xf (THz)<br>$\tau_f$(ppm/°C) | | |
|---|---|---|---|---|---|---|
| sintering temp (°C) | Ba | Sr | Ca | Ba | Sr | Ca |
| | | | | 11.00 | 14.09 | 13.02 |
| 1175 | 3.78 | 5.41 | 4.46 | 23.6 | 24.3 | 66.3 |
| | | | | −18 | −53 | −65 |
| | | | | 11.03 | 14.15 | 13.17 |
| 1200 | 5.31 | 5.42 | 4.50 | 25 | 25 | 71.2 |
| | | | | −16 | −66 | −75 |
| | | | | 11.07 | 14.25 | 13.22 |
| 1225 | 5.50 | 5.44 | 4.51 | 20 | 26.3 | 78.5 |
| | | | | −14 | −57 | −79 |
| | | | | 11.61 | 14.31 | 13.23 |
| 1250 | 5.62 | 5.48 | 4.53 | 17 | 27.4 | 81 |
| | | | | −24 | −61 | −81 |
| | | | | 12.25 | 14.26 | 13.19 |
| 1275 | 5.76 | 5.42 | 4.50 | 15 | 26.3 | 78 |
| | | | | −30 | −60 | −86 |
| | | | | - | 14.00 | 13.00 |
| 1300 | 5.80 | 5.32 | 4.40 | - | 24 | 72 |
| | | | | - | −62 | −84 |

a fixed-angle specular reflectance accessory (external incidence angle of 11.5°). In the mid-infrared region (500 to 4000 cm$^{-1}$) we used a SiC glow-bar lamp as infrared source, a Ge-coated KBr beamsplitter, and an $LN_2$-cooled HgCdTe detector. In the far-infrared range (50−600 cm$^{-1}$), we employed a mercury-arc lamp, a 6 $\mu$m coated Mylar hypersplitter, and an LHe-cooled Si-bolometer. The sample's surfaces were polished to an optical grade (0.25 $\mu$m) before the measurements. A gold mirror was used as the reference. The data were collected at a pressure of $10^{-4}$ bar and a frequency resolution of 2 cm$^{-1}$. The reflectivity spectra were evaluated by means of standard Kramers−Krönig analysis and adjusted by an oscillator model. A generalized four-parameter oscillator model was used rather than the classical model to achieve a good fit with a minimum number of physically meaningful oscillators.

## Results

**Microstructure and MW Properties.** Table 1 depicts the bulk density of $A_2MgTeO_6$ ceramics with additions of $B_2O_3$ as a function of sintering temperature. It was verified that the sinterability after $B_2O_3$ addition was greatly enhanced, as the samples showed poor densification above 1150 °C. It was found that as the sintering temperature of the ceramics $Sr_2MgTeO_6$ and $Ca_2MgTeO_6$ increases, the density improves slightly and reaches a maximum of 5.48 and 4.53 g/cm$^3$, respectively, at 1250 °C (corresponding to 96.1 and 96.4% of the theoretical densities). Any further increase in temperature decreases the density. For $Ba_2MgTeO_6$ ceramics, density increases with sintering temperature and stabilizes at around 1300 °C (90% of the theoretical value). The microstructures of 0.2 wt % $B_2O_3$-added $Ba_2MgTeO_6$, $Sr_2MgTeO_6$, and $Ca_2MgTeO_6$ ceramics sintered at 1250 °C for 4 h are shown in Figure 1. Both $Ba_2MgTeO_6$ (Figure 1a) and $Sr_2MgTeO_6$ (Figure 1b) materials have uniform distribution of grains without secondary phases. $Sr_2MgTeO_6$ ceramics are denser and have slightly larger grains (>5 $\mu$m) compared to $Ba_2MgTeO_6$ (>3 $\mu$m). On the other hand, the grain boundaries for the $Ca_2MgTeO_6$ samples (Figure 1c) are not well revealed. This is probably because of the liquid-phase sintering and higher porosity, caused by the melting of $B_2O_3$ during processing.

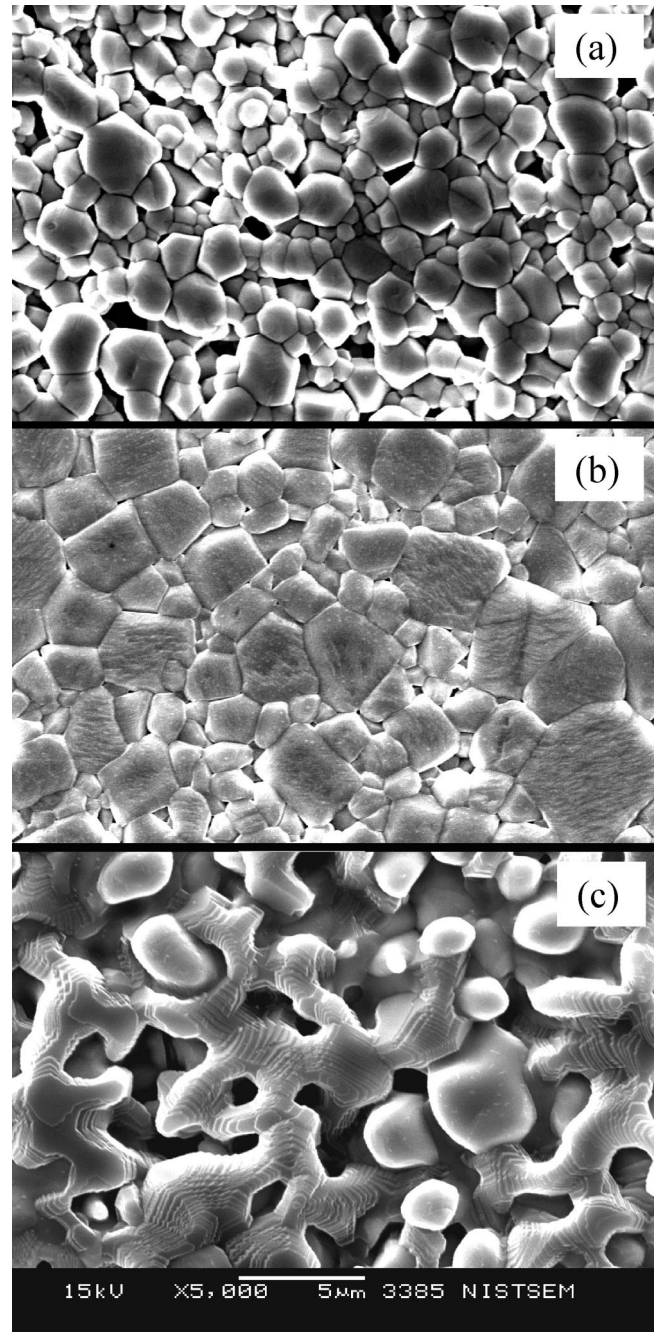


**Figure 1.** Microstructures of the (a) $Ba_2MgTeO_6$ (b) $Sr_2MgTeO_6$, and (c) $Ca_2MgTeO_6$ samples sintered at 1250 °C for 4 h.

General XRD profiles of $A_2MgTeO_6$ ceramics are given in Figure 2. The XRD pattern of $Ba_2MgTeO_6$ and $Sr_2MgTeO_6$ ceramics were tentatively indexed based on ICDD files #16-0550 and #16-0549, respectively (both cubic structures). According to Bayer,[22] these ceramics belong to $Fm\bar{3}m$ (No. 225) symmetry. The lattice parameters were then calculated assuming a cubic symmetry for both $Ba_2MgTeO_6$ and $Sr_2MgTeO_6$ ceramics, and the results ($a$ = 8.11 Å for Ba, and $a$ = 7.89 Å for Sr) were in agreement with an earlier preliminary report.[22] For $Ca_2MgTeO_6$ ceramics, a structure with lower symmetry was observed, confirming the general prediction of Bayer.[22] Prior et al.[28] studied tellurium-based

(28) Prior, T. J.; Couper, V. J.; Battle, P. D. *J. Solid State Chem.* **2005**, *178*, 153.

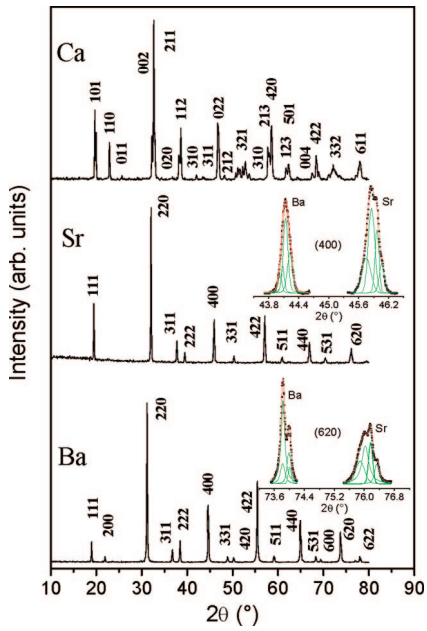


**Figure 2.** XRD patterns for the $A_2MgTeO_6$ (A = Ba, Sr, and Ca) ceramics sintered at 1250 °C for 4 h. Insets: high resolution data for the peaks (400) and (620) in Ba- and Sr-based materials (red and green lines are guides for the eyes after fitting with Gaussians).

double perovskites and start their indexing with a previously reported orthorhombic model (*Pmm*2 space group). For our $Ca_2MgTeO_6$ samples, a first tentative study showed similar results to those of Prior et al.[28] for an orthorhombic symmetry, indexed with the ICDD file #47-0026. Assuming this crystal structure, the lattice parameters were found to be $a = 7.72$ Å, $b = 5.46$ Å, and $c = 5.50$ Å.

The stability of complex perovskite structures can be well explained with the use of tolerance factors ($t$), as given by refs 1 and 7, for example. Shannon's ionic radii[29] are frequently employed to determine the tolerance factors. For all the materials studied here, the tolerance factors were in the range of a stable perovskite ($0.88 < t < 1.05$). The tolerance factors for both $Ba_2MgTeO_6$ ($t = 1.04$) and $Sr_2MgTeO_6$ ($t = 0.98$) ceramics are close to unity (characteristic of cubic or pseudocubic structures). On the other hand, it is worth to note that $Ca_2MgTeO_6$ has a tolerance factor of 0.95, which indicates a material with lower symmetry.[1,7] For this sample, spectroscopic data (discussed in the next section) help us to determine the exact symmetry as monoclinic, instead of orthorhombic, as also verified by Prior et al. in $Sr_2CaTeO_6$ ceramics.[28] Based on previous results of Dias et al.,[30] which showed how to distinguish between cubic or pseudocubic symmetries in similar Ba- and Sr-based double perovskites, high resolution XRD analyses were then carried out on the particular peaks (400) and (620). The results are displayed as insets in Figure 2, showing that the materials presented splitting of the XRD peaks, which is more unequivocal in Sr-based ceramics. The experimental data were fitted by pseudo-Voigt curves (green lines) only to facilitate the visualization. These results confirm a tetragonal distortion in the cubic lattices for both Ba- and Sr-based materials, as also verified in indium-containing double perovskites studied by Dias et al.[30] As it will be showed later, these observations are confirmed by the spectroscopic data.

The results for the microwave dielectric properties of $A_2MgTeO_6$ ceramics with sintering temperature are shown in Table 1. It was found that $\varepsilon_r$ and $Q_u$xf increases with temperature reaching a maximum at about 1250 °C for $Sr_2MgTeO_6$ and $Ca_2MgTeO_6$ ceramics. Any further increase in the sintering temperature deteriorates the microwave properties. It appears that the variation in the microwave dielectric properties is directly correlated with the behavior of the density of the samples. Exaggerated grain growth coupled with a decrease in density that occurred at elevated temperatures for these samples are probably the reasons for the degradation of the microwave properties. Ceramics with Ba presented a continuous increasing behavior with temperature for $\varepsilon_r$; however, $Q_u$xf decreased when sintered above 1200 °C. The $\tau_f$ values of the $Sr_2MgTeO_6$ ceramics are nearly the same for all sintering temperatures, whereas those of $Ca_2MgTeO_6$ materials increased and then have stabilized around −84 ppm/°C at higher temperatures. At 1250 °C (assumed as the optimum sintering temperature), $Sr_2MgTeO_6$ and $Ca_2MgTeO_6$ samples exhibited the following values for the microwave dielectric properties: 14.3 and 13.2 for $\varepsilon_r$, 27.4 and 81 THz ($Q_u$xf), and $\tau_f$ equal to −61 and −81 ppm/°C. The best properties for $Ba_2MgTeO_6$ samples were $\varepsilon_r = 11$, $Q_u$xf = 25 THz, and $\tau_f = -16$ ppm/°C, obtained at 1200 °C. For this ceramic, the subsequent increase in the sintering temperature degraded the microwave properties and the specimen showed no resonance after sintering at 1300 °C. Among the three complex magnesium tellurates investigated, the highest quality factor was obtained for $Ca_2MgTeO_6$ ceramics sintered at 1250 °C (81 THz).

Several reports are available in the literature correlating $t$ and $\tau_f$.[1,7] However, the establishment of a relationship between $\tau_f$ and crystal structure in complex perovskites is not an easy task. Despite of that, Reaney and Iddles[7] provided an empirical relationship between $\tau_f$ and $t$ for many perovskite compounds. For the materials investigated here, $t$ increased from 0.95 ($Ca_2MgTeO_6$), reaches 0.98 ($Sr_2MgTeO_6$), and finally assumes the value 1.04 ($Ba_2MgTeO_6$). Reaney's empirical relation between $\tau_f$ and $t$ shows three distinct regions relative to the distortions (tilts) of the oxygen octahedra:[7] in-phase concurrent with antiphase tilts ($t > 0.97$), antiphase tilting ($0.97 > t > 0.99$), and untilted ($0.99 > t > 1.05$) structures. The temperature coefficient of resonant frequency ($\tau_f$) of the microwave ceramics depends on the temperature coefficient of dielectric constant ($\tau_\epsilon$) and on the linear coefficient of thermal expansion ($\alpha_L$), according to the relation given in ref 7. For complex perovskite materials, $\alpha_L$ usually lies between 9 and 12 ppm/°C. Also, according to Reaney and Iddles,[7] for $\tau_\epsilon$ values higher than positive 50 ppm/°C, the observed tolerance factors are lower than 0.97. For $Ca_2MgTeO_6$, $t = 0.95$ and $\tau_f = -81$ ppm/°C. Hence, it is expected for $Ca_2MgTeO_6$ ceramics highly positive $\tau_\epsilon$ values. $Sr_2MgTeO_6$ presents $t = 0.98$, which is in the region of antiphase tilting. There are a lot of materials

(29) Shannon, R. D. *Acta Crystallogr., Sect. A: Found. Crystallogr.* **1976**, *32*, 751.
(30) Dias, A.; Khalam, L. A.; Sebastian, M. T.; Moreira, R. L. *J. Solid State Chem.* **2007**, *180*, 2143.

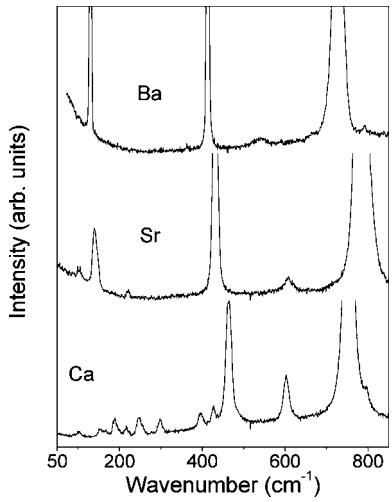


**Figure 3.** Room temperature Raman spectra for the $A_2MgTeO_6$ (A = Ba, Sr, and Ca) complex perovskites.

in this region with both positive and negative $\tau_\epsilon$ with a wide range of resulting positive and negative $\tau_f$ values. Hence, the negative $\tau_f$ of $Sr_2MgTeO_6$ ceramics (−61 ppm/°C) could be related to its tolerance factor, once we can predict a high positive $\tau_\epsilon$ value for this ceramic (∼100 ppm/°C). It is interesting to note that $Ba_2MgTeO_6$ ceramics would occur in the untilted region ($t = 1.04$). In this region, $\tau_\epsilon$ and hence $\tau_f$ approaches zero as the tolerance factor approaches 1.05. However, $Ba_2MgTeO_6$ has a $\tau_f$ of −16 ppm/°C. The increase in $\tau_f$ can be due to the addition of 0.2 wt % $B_2O_3$ (it is well-known that most of the glasses have negative $\tau_f$). Thus, the marginal disagreement between the $\tau_f$ and the t values, corresponding to that reported by Reaney and Iddles,[7] could be due to the addition of $B_2O_3$.

**Raman scattering and Infrared Reflectivity Spectra.** Room-temperature Raman analysis was carried out in $Ba_2MgTeO_6$, $Sr_2MgTeO_6$, and $Ca_2MgTeO_6$ materials, and the results are displayed in Figure 3. As it can be seen, two different spectral profiles are clearly observed, which indicates that the ceramics likely occur in different structures. Dominating bands centered at 130, 410, and 725 $cm^{-1}$ are present in Ba samples, while in Sr-based ceramics the corresponding bands occur in the frequencies 140, 430, and 785 $cm^{-1}$. These results were previously observed in similar 1:1 ordered ceramics.[31,32] Ca-based perovskites showed phonon modes centered in similar positions besides many additional strong bands in the region 150−400 $cm^{-1}$, associated with its lower-symmetry structure. As a general trend, the bands of the $Sr_2MgTeO_6$ ceramics are up-shifted compared to their Ba analogues. This is as a consequence of the smaller Sr ions compared to Ba ions, which leads to a contracted unit cell, with smaller ionic distances and, then, to general stronger ionic bonds. Similar behavior occurred for Ca-based samples, although a more complex analysis must be done because this material belongs to a different crystal structure.

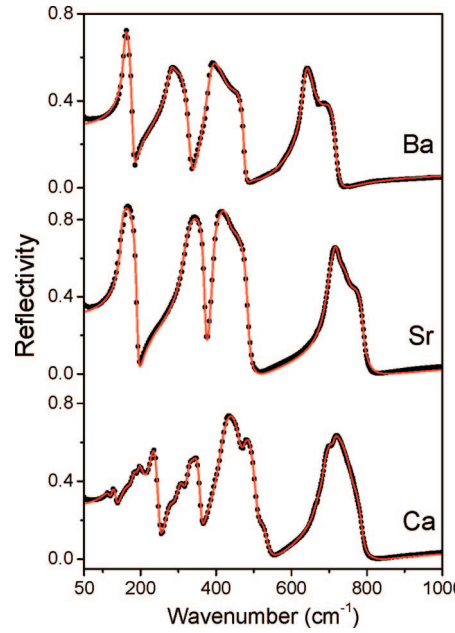


**Figure 4.** Measured (square symbols) and adjusted (solid line) infrared reflectivity spectra for the $A_2MgTeO_6$ (A = Ba, Sr, and Ca) ceramics.

The infrared reflectivity spectra of $Ba_2MgTeO_6$, $Sr_2MgTeO_6$, and $Ca_2MgTeO_6$ materials are presented in Figure 4. The visual inspection of the spectra shows at least 6 well-defined modes for Ba- and Sr-based samples, while for $Ca_2MgTeO_6$ one can observe a minimum of 13 bands. Notice the high similarity between the spectra of Ba and Sr ceramics, confirming their average noncubic symmetry, as it will be discussed later. A careful inspection of Figure 4 reveals the presence of other weak bands and shoulders in all samples. In view of that, a group-theory investigation was undertaken toward a better understanding of the crystal chemistry of these samples. The exact number of bands will be known only after a precise fitting by using theoretical approaches.

**Group-Theoretical Analysis and Discussions.** The ideal simple perovskite is cubic, space group $Pm\bar{3}m$, but tilting of the oxygen octahedra is regularly found usually driven by a mismatch in the size of the cations (it is worthy noticing that there are no-active first-order Raman phonons and only three infrared-active modes for the ideal $Pm\bar{3}m$ group). For complex cubic perovskites of general formula $A_2B'B''O_6$, a $Fm\bar{3}m$ symmetry ($O_h^5$, No. 225, Glazer's notation $a^0a^0a^0$) is frequently expected in ordered, untilted lattices. This configuration allows a classification of the normal modes at the Brillouin zone-center as $\Gamma = A_g \oplus E_g \oplus F_{1g} \oplus 2\ F_{2g} \oplus 5\ F_{1u} \oplus F_{2u}$. The symmetry analysis of the irreducible representations above indicates that 4 modes are Raman-active ($A_g$, $E_g$, 2 $F_{2g}$), and also 4 modes are infrared-active (4 $F_{1u}$).[33] For $Ba_2MgTeO_6$ and $Sr_2MgTeO_6$ ceramics, XRD data showed that a $Fm\bar{3}m$ structure is not adequate because of the splitting of (400) and (620) peaks, verified after high resolution investigations. It is believed that a structure with lower symmetry is more plausible for these materials, in particular, the tetragonal $I4/m$ structure, as previously determined for other similar ceramics.[23,30]

(31) Dias, A.; Khalam, L. A.; Sebastian, M. T.; Paschoal, C. W. A.; Moreira, R. L. *Chem. Mater.* **2006**, *18*, 214.
(32) Moreira, R. L.; Khalam, L. A.; Sebastian, M. T.; Dias, A. *J. Eur. Ceram. Soc.* **2007**, *27*, 2803.
(33) Rousseau, D. L.; Bauman, R. P.; Porto, S. P. S. *J. Raman Spectrosc.* **1981**, *10*, 253.

Thus, as also carried out by Dias et al. in $Ba_2InTaO_6$ samples,[30] a rigorous assessment of the Raman spectra (Figure 3) was conducted, and the results showed that the materials present a larger number of features than the three dominating Raman-active modes. Then, we take the previous results developed by Dias et al.[30] to help us to start a new group-theory analysis in a more realistic basis. Assuming their conclusions for a tetragonal structure, set in space group *I*4/*m* (No. 87), $Ba_2MgTeO_6$ and $Sr_2MgTeO_6$ materials could be described as belonging to the $C_{4h}^5$ space-group (Glazer's notation $a^0a^0c^-$). This tetragonal structure is derived from the prototype $Fm\bar{3}m$ cubic structure by an antiphase tilt of $MgO_6$ and $TeO_6$ octahedra in the basal plane along the [001] direction of the cubic cell. For this structure, the Ba or Sr atoms occupy 4*d* sites of $S_4$ symmetry, the Mg and Te ions occupy 2*a* and 2*b* sites of $C_{4h}$ symmetry, and the oxygen atoms are in the 8*h* and 4*e* sites (*Cs* and $C_4$ symmetries, respectively). Then, using the site group method of Rousseau et al.,[33] it is possible to obtain the following distribution in terms of the irreducible representations of the $C_{4h}$ point group as $\Gamma = 3A_g \oplus 5A_u \oplus 3B_g \oplus B_u \oplus 3E_g \oplus 6E_u$.[31] Excluding the acoustic ($A_u \oplus E_u$) and silent modes ($B_u$), we would expect 9 Raman-active modes ($3A_g$, $3B_g$, $3E_g$) and 9 infrared bands ($4A_u$, $5E_u$) for this structure.

For $Ca_2MgTeO_6$ ceramics, we shall assume the monoclinic structure, space group $P2_1/n$ ($C_{2h}^5$, No. 14, Glazer's notation $a^-a^-c^+$), according to the suggestions of other authors that studied similar materials, including Te-based ceramics.[19,23,30] The monoclinic $P2_1/n$ structure can be understood as resulting from a combination of in-phase (+) and antiphase (−) tilts of $MgO_6$ and $TeO_6$ octahedra in the (−−+) sense about the axes of the ideal cubic perovskite. In this case, Mg and Te ions should occupy the 2*a* and 2*b* Wyckoff-sites of both $C_i$ symmetry, and Ca and O ions would be in 4*e* sites of general $C_1$ symmetry. The site group method leads now to the following distribution of irreducible representations of the $C_{2h}$ point group:[30] $\Gamma = 12A_g \oplus 12B_g \oplus 18A_u \oplus 18B_u$. Thus, one would have 24 Raman-active phonon modes ($12A_g$, $12B_g$) and 33 infrared-active modes ($17A_u$, $16B_u$) for this sample (the acoustic modes are $A_u \oplus 2B_u$).

Based on the above factor-group analyses, careful fitting of Raman spectra of both $Ba_2MgTeO_6$ and $Sr_2MgTeO_6$ samples were carried out. The results for Ba- and Sr-based compounds are displayed in Figures 5 and 6. For the Ba-based sample, the experimental data are rather scattered, particularly for the low-frequency region, which sometimes makes it difficult to have the correct adjustment of the spectrum. The final fittings (red lines in Figures 5 and 6) were obtained through a sum of 9 Lorentzian lines, in perfect agreement with the theoretical predictions. Table 2 presents the parameters after deconvolution of the spectrum of $Ba_2MgTeO_6$ and $Sr_2MgTeO_6$, i.e., wavenumbers ($cm^{-1}$) and full width at half-maxima ($cm^{-1}$) for the phonon modes identified on the experimental data. As a general trend, the bands in Ba samples are down-shifted in comparison with Sr ceramics, which are directly related to their smaller ionic radii and, consequently, stronger bonds. The present results lead us to conclude that the correct structure for the $Ba_2MgTeO_6$ and $Sr_2MgTeO_6$ perovskites appears to be within the tetragonal *I*4/*m* ($C_{4h}^5$) space group.

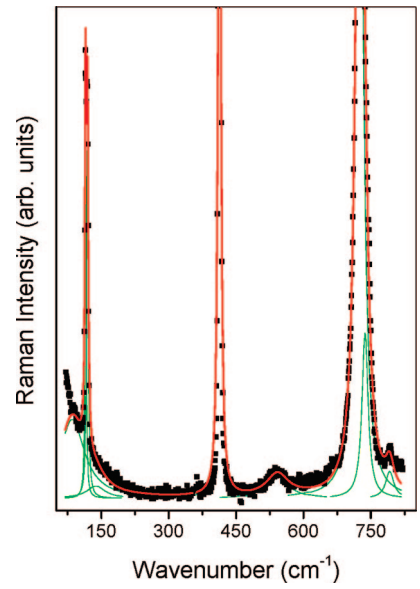


**Figure 5.** Raman spectra for $Ba_2MgTeO_6$ ceramics. Experimental data are in solid squares while the fitting curve is the red line. Green lines represent the phonon modes adjusted by Lorentzian curves.

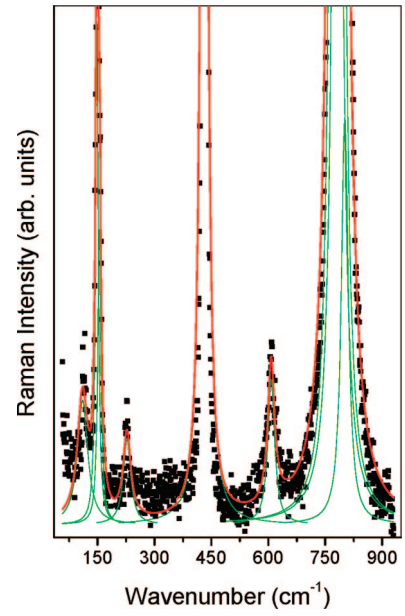


**Figure 6.** Raman spectra for $Sr_2MgTeO_6$ ceramics. Experimental data are in solid squares while the fitting curve is the red line. Green lines represent the phonon modes adjusted by Lorentzian curves.

Figure 7 presents the Raman spectra for the $Ca_2MgTeO_6$ perovskite. Experimental data did not scatter as for $Ba_2MgTeO_6$ materials, which was beneficial for the analysis conducted in the spectrum obtained at room-temperature. The dashed line centered at 332 $cm^{-1}$ denotes a changing in the intensity scale used for better visualization. The fitting was performed, and 20 Lorentzian lines could be depicted, in good agreement with the hypothesis for a monoclinic $P2_1/n$ ($C_{2h}^5$) structure, where 24 phonon modes were foreseen. Table 2 also presents the parameters of this sample after deconvolution of the spectrum for the phonon modes identified on the experimental data. Ca-based complex perovskites are

**Table 2. Observed Raman Modes for the $A_2MgTeO_6$ Ceramics[a]**

| | $Ba_2MgTeO_6$ | | $Sr_2MgTeO_6$ | | $Ca_2MgTeO_6$ | |
|---|---|---|---|---|---|---|
| band | Ω | γ | Ω | γ | Ω | γ |
| 1 | 100.0 | 29 | 101.0 | 33 | 88.5 | 24 |
| 2 | 127.9 | 3 | 138.9 | 9 | 103.2 | 12 |
| 3 | 131.8 | 4 | 145.4 | 10 | 153.7 | 11 |
| 4 | 149.3 | 56 | 221.6 | 24 | 166.6 | 7 |
| 5 | 412.9 | 6 | 431.5 | 12 | 188.3 | 9 |
| 6 | 544.5 | 57 | 607.6 | 22 | 196.0 | 10 |
| 7 | 724.2 | 18 | 777.9 | 17 | 212.7 | 4 |
| 8 | 737.2 | 17 | 786.6 | 19 | 217.4 | 6 |
| 9 | 794.4 | 21 | 802.8 | 23 | 245.0 | 5 |
| 10 | | | | | 250.7 | 11 |
| 11 | | | | | 278.0 | 3 |
| 12 | | | | | 298.5 | 10 |
| 13 | | | | | 308.9 | 14 |
| 14 | | | | | 396.2 | 18 |
| 15 | | | | | 426.8 | 8 |
| 16 | | | | | 463.6 | 14 |
| 17 | | | | | 471.4 | 43 |
| 18 | | | | | 603.1 | 19 |
| 19 | | | | | 752.6 | 13 |
| 20 | | | | | 797.2 | 11 |

[a] Positions (Ω, $cm^{-1}$) and full width at half-maxima (γ, $cm^{-1}$) were obtained from the adjustment of the experimental data by Lorentzian lines.

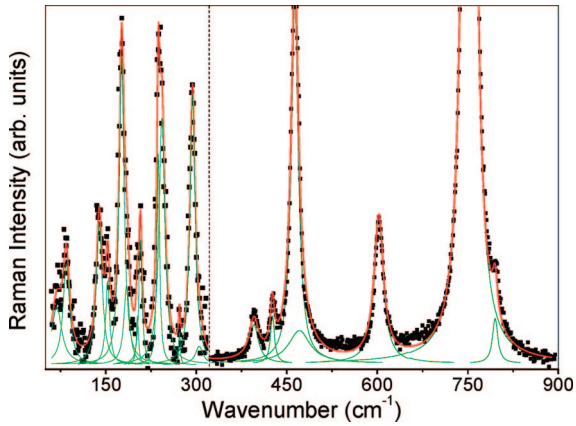


**Figure 7.** Raman spectra for $Ca_2MgTeO_6$ ceramics. Experimental data are in solid squares while the fitting curve is the red line. Green lines represent the phonon modes adjusted by Lorentzian curves. The dashed line centered at 332 $cm^{-1}$ denotes a changing in the intensity scale used for better visualization.

frequently found to belong to lower-symmetry structures because of the smaller Ca ions compared with the analogous Ba- or even Sr-containing perovskites, which lead to distorted (tilted) structures.[34,35]

Now, the results from infrared reflectivity measurements will be discussed. The spectra displayed in Figure 4 were analyzed by using the four-parameter semiquantum model,[36] using a nonlinear least-squares program.[37] According to this model, the infrared phonon contributions to the complex dielectric function $\varepsilon(\omega)$ are given by:

$$\varepsilon(\omega) = \varepsilon_\infty \prod_{j=1}^{N} \frac{\Omega_{j,\mathrm{LO}}^2 - \omega^2 + i\omega\gamma_{j,\mathrm{LO}}}{\Omega_{j,\mathrm{TO}}^2 - \omega^2 + i\omega\gamma_{j,\mathrm{TO}}} \qquad (1)$$

where $\varepsilon_\infty$ is the dielectric constant due to the electronic polarization contribution, $\Omega_{j,\mathrm{LO}}(\Omega_{j,\mathrm{TO}})$ and $\gamma_{j,\mathrm{LO}}(\gamma_{j,\mathrm{TO}})$ are the frequency and damping of the $j$-th longitudinal (transverse) optical modes, respectively. $N$ is the number of polar phonons. At quasinormal incidence, the dielectric function is related to the optical reflectance $R$ by the Fresnel formula:

$$R = \left|\frac{\sqrt{\varepsilon(\omega)} - 1}{\sqrt{\varepsilon(\omega)} + 1}\right|^2 \qquad (2)$$

Equations 1 and 2 were used to fit the experimental data, and the results are presented in Figure 4 as solid red curves. Then, we could obtain the wavenumbers and widths of the transverse (TO) and longitudinal (LO) infrared modes, which are listed in Table 3 for all materials. We note first that 9 infrared modes were discerned for both Ba- and Sr-based ceramics, while 17 modes could be adjusted for $Ca_2MgTeO_6$. The agreement between observed and predicted number of modes for the materials with tetragonal structure is remarkable. Concerning the Ca-based ceramic, the situation is quite similar to those of REMgB"$O_6$ (RE = rare earth; B″ = Ti,

**Table 3. Dispersion Parameters Calculated from The Fit of the Infrared Reflectance Spectrum of $A_2MgTeO_6$ [a]**

| $\Omega_{j,\mathrm{TO}}$ | $\gamma_{j,\mathrm{TO}}$ | $\Omega_{j,\mathrm{LO}}$ | $\gamma_{j,\mathrm{LO}}$ | $\Delta\epsilon_j$ | $10^5 \tan\delta_j/\omega$ |
|---|---|---|---|---|---|
| $Ba_2MgTeO_6$ | | | | | |
| 157.6 | 8.3 | 180.1 | 11.8 | 3.075 | 9.433 |
| 278.9 | 19.3 | 285.0 | 26.5 | 1.520 | 3.475 |
| 291.6 | 43.5 | 333.3 | 18.7 | 1.296 | 6.100 |
| 382.8 | 20.1 | 433.8 | 79.5 | 1.085 | 1.373 |
| 445.8 | 66.2 | 475.4 | 11.9 | 0.120 | 0.369 |
| 479.7 | 42.0 | 489.4 | 79.2 | 0.010 | 0.017 |
| 618.1 | 72.6 | 632.6 | 88.5 | 0.299 | 0.522 |
| 632.7 | 15.6 | 652.4 | 83.3 | 0.001 | 0.000 |
| 693.6 | 66.9 | 718.4 | 18.0 | 0.095 | 0.122 |
| $\varepsilon_\infty = 3.355$ | | $\epsilon_r = 10.856$ | | $\Sigma \tan\delta_j/\omega = 21.4 \times 10^{-5}$ | |
| $Sr_2MgTeO_6$ | | | | | |
| 150.8 | 7.3 | 192.3 | 7.0 | 5.813 | 14.295 |
| 320.8 | 19.6 | 328.1 | 26.1 | 3.044 | 4.410 |
| 328.2 | 20.6 | 372.7 | 11.6 | 0.040 | 0.058 |
| 392.2 | 11.0 | 447.8 | 28.3 | 0.590 | 0.322 |
| 449.1 | 28.2 | 485.9 | 12.5 | 0.011 | 0.012 |
| 611.1 | 43.1 | 614.1 | 45.3 | 0.034 | 0.030 |
| 691.3 | 49.9 | 700.3 | 50.8 | 0.433 | 0.344 |
| 701.0 | 19.3 | 749.9 | 69.8 | 0.029 | 0.009 |
| 766.5 | 68.5 | 790.3 | 13.4 | 0.033 | 0.029 |
| $\varepsilon_\infty = 3.115$ | | $\epsilon_r = 13.141$ | | $\Sigma \tan\delta_j/\omega = 19.5 \times 10^{-5}$ | |
| $Ca_2MgTeO_6$ | | | | | |
| 120.2 | 14.8 | 120.5 | 11.0 | 0.105 | 1.033 |
| 129.8 | 15.1 | 134.9 | 15.8 | 1.069 | 9.261 |
| 165.3 | 36.0 | 180.3 | 39.0 | 1.749 | 22.223 |
| 182.2 | 14.9 | 182.3 | 33.6 | 0.001 | 0.005 |
| 196.7 | 14.1 | 196.7 | 27.5 | 0.001 | 0.002 |
| 229.8 | 19.2 | 249.3 | 14.2 | 1.275 | 4.477 |
| 276.4 | 20.6 | 278.7 | 28.2 | 0.110 | 0.286 |
| 305.7 | 20.2 | 313.6 | 29.7 | 0.407 | 0.851 |
| 327.2 | 15.2 | 327.5 | 33.3 | 0.014 | 0.019 |
| 346.3 | 27.0 | 359.6 | 14.3 | 0.552 | 1.198 |
| 414.7 | 25.6 | 466.1 | 31.1 | 1.475 | 2.113 |
| 472.2 | 29.5 | 507.8 | 24.4 | 0.085 | 0.108 |
| 519.5 | 29.2 | 533.9 | 28.7 | 0.033 | 0.034 |
| 677.7 | 16.8 | 677.7 | 13.8 | 0.001 | 0.001 |
| 681.9 | 26.9 | 711.2 | 10.0 | 0.517 | 0.289 |
| 711.4 | 9.5 | 765.1 | 48.0 | 0.003 | 0.001 |
| 774.3 | 42.0 | 783.5 | 18.2 | 0.005 | 0.004 |
| $\varepsilon_\infty = 2.968$ | | $\epsilon_r = 10.371$ | | $\Sigma \tan\delta_j/\omega = 41.9 \times 10^{-5}$ | |

[a] The positions (Ω) and damping constants (γ) are given in $cm^{-1}$.

(34) Ting, V.; Liu, Y.; Withers, R. L.; Norén, L.; James, M.; Fitzgerald, J. D. *J. Solid State Chem.* **2006**, *179*, 551.
(35) Fu, W. T.; Ijdo, D. J. W. *Solid State Commun.* **2005**, *134*, 177.
(36) Gervais, F.; Echegut, P. In *Incommensurate phases in dielectrics*; Blinc, R., Levanyuk, A. P., Eds.; North Holland: Amsterdam, 1986; p 337.
(37) Meneses, D. D.; Gruener, G.; Malki, M.; Echegut, P. *J. Non-Cryst. Solids* **2005**, *351*, 124.

Sn) compounds, where quasi-accidental degeneracy forbids the distinction between corresponding $A_u$ and $B_u$ modes, and also only 17 infrared modes are observed instead of the 33 foreseen ones ($17A_u$, $16B_u$).[38–40] It is also worth noticing the resemblance of the spectra of our $Ca_2MgTeO_6$ compound and those of $REMgB''O_6$ of refs 38–40, which derives from the fact that the vibrational modes come essentially from the $MgO_6$ and $B''O_6$ octahedra, as tentatively assigned in those references.

Once the infrared modes were determined, the oscillator strengths of the individual *j*-th TO modes can be obtained (Table 3) by:

$$\Delta\varepsilon_j = \frac{\varepsilon_\infty}{\Omega_{j,\mathrm{TO}}^2} \times \frac{\prod_k (\Omega_{k,\mathrm{LO}}^2 - \Omega_{j,\mathrm{TO}}^2)}{\prod_{k\neq j} (\Omega_{k,\mathrm{TO}}^2 - \Omega_{j,\mathrm{TO}}^2)}. \quad (3)$$

Now, the static (infrared) dielectric constant, which corresponds to the intrinsic MW dielectric constant, can be obtained by adding the oscillator strengths over all modes according to the equation:

$$\varepsilon_r = \varepsilon_\infty + \sum_{j=i}^{N} \Delta\varepsilon_j \quad (4)$$

The values of$\varepsilon_r$, and $\varepsilon_\infty$ for all materials are given in Table 3, together with the phonon modes. It is important to note that the intrinsic unloaded quality factor at MW region, $Q_u$, can be calculated as the reciprocal of the dielectric loss tangent (tan $\delta$), in the limit where $\Omega_{j,\mathrm{TO}} \gg \omega$, which leads to

$$\tan\delta = \sum_j \tan\delta_j = \sum_j \omega \frac{\Delta\varepsilon_j \gamma_{j,\mathrm{TO}}}{\varepsilon_r \Omega_{j,\mathrm{TO}}^2} \quad (5)$$

The values for $\sum_j \tan\delta_j/\omega$ are also presented in Table 3. The values for the intrinsic (FTIR) quality factors times frequency were, respectively, 140, 154, and 72 THz for Ba-, Sr-, and Ca-based ceramics. Intrinsic $\varepsilon_r$ is in good agreement with the MW measurements (Tables 1 and 3). However, the intrinsic $Q_u$xf is clearly higher than the extrinsic one (MW) for Ba- and Sr-based materials, showing that the dielectric losses at MW are mainly extrinsic. This higher value is one due to the extrapolation of the infrared losses to the MW region, which is often spoiled because of the dominance of extrinsic losses of different origins (polar species, microstructural defects, etc.), leading to overestimated quality factors.[41–43] Particularly for the $Ca_2MgTeO_6$ sample, a lower value was found for this merit factor and can be attributed to the number of modes found during fitting. In this respect, the low number of bands is related to the proximity of the TO modes of different irreducible representations, which makes their assessment and determination difficult by regular fitting procedures. As a consequence, the bandwidths become overestimated, reducing the projected quality factor. Despite that, extrinsic and intrinsic quality factors agree well for this material. A previous study concerning the structure−property relationship of $BaB'_{0.5}B''_{0.5}O_3$ complex-perovskite materials has been reported by Zurmühlen et al.[42,43] It was shown that the ionic size is the most important parameter, determining the tolerance factor of the structural packing and hence controlling the phonon energies and their damping as well as intrinsic permittivity and loss.

Howard et al.[44] have used group-theoretical methods to enumerate the structures of ordered double perovskites by considering different combinations of octahedral tilting starting from the cubic $Fm\bar{3}m$ structure. This structure is a result of the doubling of the ideal perovskite by imposition of rock-salt 1:1 ordering. Tilting of the $BO_6$ octahedra are allowed and hence lower-symmetry structures would result. Howard et al.[44] found 11 lower-symmetry structures derived from the $Fm\bar{3}m$ cubic space group as a result of the cation ordering in combination with the corner-linked tilting of the octahedral units. Group−subgroup relationships were established and help us to explain the experimentally observed structures in $A_2MgTeO_6$ perovskites studied in the present work, as discussed below.

$Ba_2MgTeO_6$ and $Sr_2MgTeO_6$ perovskites present tolerance factors nearly the unity, which means that a cubic structure is expected. Many other complex perovskites with tolerance factors near to the unity (or traditionally considered cubic) were recently revisited and distorted structures were determined.[30,31] Dias et al.[30,31] showed that although XRD and other techniques indicate cubic or nearly cubic structures, Raman-spectroscopic analysis demonstrated tetragonal structures for double perovskite materials. According to the Glazer notation,[41] the $I4/m$ structure derives from the $Fm\bar{3}m$ ($a^0a^0a^0$) by a single rotation of the $BO_6$ octahedra about one of the four-fold axes, lowering the symmetry to tetragonal ($a^0a^0c^-$). This structure presents nine Raman-active bands and nine infrared-active phonon modes,[31,33] which is compatible with our findings for both $Ba_2MgTeO_6$ and $Sr_2MgTeO_6$ perovskites. We believe that the small tetragonal distortion in these materials, particularly in Ba-based ceramics, is similar to that observed in $Ba_2YNbO_6$,[31] i.e., the octahedral tilting is too small to be detected by XRD or even more sophisticated techniques, like neutrons and electron diffraction. However, the antiphase distortions appear to be sufficiently large to be detected by Raman and infrared spectroscopies.

## Conclusions

$A_2MgTeO_6$ (A = Ba, Sr, Ca) ceramics were prepared as single-phase materials and their microstructure, microwave dielectric properties, and vibrational features are reported for the first time. The ceramics showed potential characteristics for applications as dielectric resonators; particularly, the temperature coefficients of resonant frequencies are found

(38) Salak, A. N.; Khalyavin, D. D.; Ferreira, V. M.; Ribeiro, J. L.; Vieira, L. G. *J. Appl. Phys.* **2006**, *99*, 094104.
(39) Babu, G. S.; Subramanian, V.; Murthy, V. R. K.; Lin, I. N.; Chia, C. T.; Liu, H. L. *J. Appl. Phys.* **2007**, *102*, 064906.
(40) Babu, G. S.; Subramanian, V.; Murthy, V. R. K.; Moreira, R. L.; Lobo, R. P. S. M. *J. Appl. Phys.* **2008**, *103*, 084104.
(41) Petzelt, J.; Kamba, S. *Mater. Chem. Phys.* **2003**, *79*, 175.
(42) Zurmühlen, R.; Petzelt, J.; Kamba, S.; Voitsekhovskii, V.; Colla, E.; Setter, N. *J. Appl. Phys.* **1995**, *77*, 5341.
(43) Zurmühlen, R.; Petzelt, J.; Kamba, S.; Kozlov, G.; Volkov, A.; Gorshunov, B.; Dube, D.; Tagantsev, A.; Setter, N. *J. Appl. Phys.* **1995**, *77*, 5351.
(44) Howard, C. J.; Kennedy, B. J.; Woodward, P. M. *Acta Crystallogr.* **2003**, *B59*, 463.

to be related to the tolerance factors, which is a significant parameter for perovskite structures. Together with XRD technique, experimental Raman and infrared data allowed us to determine the correct structure for $Ba_2MgTeO_6$, $Sr_2MgTeO_6$, and $Ca_2MgTeO_6$ perovskites in light of group-theoretical models. Besides, these results contributed to understand and explain small lattice distortions in materials with tolerance factors close to unity (usually considered cubic). While Ba- and Sr-based materials present a tetragonal $I4/m$ structure with small deviations from the ideal cubic structure, Ca-based ceramics belongs to a monoclinic $P2_1/n$ ($C_{2h}^5$) structure.

**Acknowledgment.** The Brazilian authors acknowledge the financial support from CNPq, FINEP, and FAPEMIG. Special thanks are directed to Prof. M. A. Pimenta (UFMG) for his hospitality during Raman experiments. G. Subodh is grateful to Council of Scientific and Industrial Research (CSIR, India) for a junior research fellowship.

CM8003326